

The development of a reagentless lactate biosensor based on a novel conducting polymer

J. Haccoun, B. Piro¹, V. Noël¹, M.C. Pham^{*,1}

Laboratoire Interfaces-Traitements-Organisation et Dynamique des Systèmes (ITODYS), de l'Université Paris 7-Denis Diderot, associé au CNRS, UMR 7086, 1 rue Guy de la Brosse, 75005 Paris, France

Received 31 May 2005; received in revised form 26 August 2005; accepted 2 September 2005
Available online 2 November 2005

Abstract

A reagentless lactate biosensor is described, based on an electropolymerized copolymer film poly(5-hydroxy-1,4-naphthoquinone-co-5-hydroxy-3-acetic acid-1,4-naphthoquinone). The quinone group, as part of the polymer backbone, is electroactive and very stable in neutral aqueous medium. It can therefore act as an immobilized mediator for the enzyme recycling, at a working potential much lower than those commonly reported in the literature for other mediators. Experimental conditions for amperometric measurements (temperature, pH) are studied, especially the interference between quinone and molecular oxygen to investigate the enzyme/quinone recycling kinetic. Some well-known interferents are shown to have no measurable effect on the amperometric curves.

© 2005 Elsevier B.V. All rights reserved.

Keywords: Conducting polymer; Lactate oxidase; Reagentless detection; Quinone; Interferents

1. Introduction

Enzyme-based amperometric biosensors are very common systems nowadays. Enzyme immobilization can be achieved through various techniques, as incorporation in carbon paste [1], in redox hydrogel [2,3], immobilized on self-assembled monolayers [4], in non-conducting [5–7] or in conducting or electroactive polymers [8–12]. In the latter cases, to construct reagentless biosensors, polymers must bear a chemically reactive group to irreversibly bind the biomolecule, and, except for direct electron transfer (ET), an electroactive group that plays the role of immobilized redox mediator between the active site of the enzyme and the electrode. It must be noticed that true direct ET, undoubtedly demonstrated for enzymes like cytochrome c [13] or dehydrogenases [14], has never been evidenced for oxidase enzymes [15,16].

Obviously, the mediators must be chosen in order to thermodynamically allow ET towards/from the active site of

the enzyme, with a sufficiently fast kinetic [16,17] and an overpotential (with respect to the formal potential of the enzymatic active site) as low as possible, to avoid interferences.

The quinone/hydroquinone couple is one of the first redox couple utilized among all mediators reported in the literature [18]. This is probably due to the fact that the quinone/hydroquinone couple is widely present in vivo in biological systems. However, drawbacks such as low stability in alkaline or even neutral media, or low ET kinetic are often recalled, compared to inorganic redox systems. On the contrary, a great advantage of quinone systems lays in their very low redox potentials. In Table 1 [19–22] are listed the most common mediators utilized with oxidase enzymes like glucose oxidase and lactate oxidase. It is very clear that the quinone function is able to shuttle electrons from the active site of an enzyme to the electrode [23,24], with lowest working potential [22].

We reported in a previous note the preliminary results on a lactate oxidase-modified electrode, based on a bifunctional copolymer poly(5-hydroxy-1,4-naphthoquinone-co-5-hydroxy-3-thioacetic acid-1,4-naphthoquinone) [25]. Herein, we study the characteristics of the bioelectrode and define the best operating conditions. It is shown that the sensor is insensitive

* Corresponding author. Tel.: +33 1 44276961; fax: +33 1 44276814.

E-mail address: MCPHAM@paris7.jussieu.fr (M.C. Pham).

¹ ISE member.

Table 1
Classical mediators for glucose oxidase or lactate oxidase (from Ref. [19])

Enzyme	Mediator	Working potential (mV vs. SCE)
Glucose oxidase	Os-PAA	360 [18]
	TTF	300
	Ferrocene carboxylic acid	285
	Os-dimethyl-bpy	200 [16]
	Ferrocene	165
	TCNQ	127
	Benzoquinone	39
	Oxygen	600
Lactate oxidase	Os-PAA	400 [18]
	Ferrocene carboxylic acid	280
	Os-dimethyl-bpy	200 [16]
	Fe(CN) ₆ ^{3−}	180
	Benzoquinone	60
	Os-dimethoxy-bpy	55 [17]
	Methylene green	30
	Methylene blue	30
	Oxygen	600

to most common interferents and can be applied to commercial food-industry samples with good reliability.

2. Experimental

2.1. Materials

5-hydroxy-1,4-naphthoquinone (juglone) was purchased from Fluka. Lactate oxidase (LOD, from *Pediococcus* species) was from Sigma Chem. Co. L(+)-lactic acid (sodium salt) was obtained from Acros. ABTS[®] is from ICN. Aqueous solutions were made with bi-distilled water. 5-hydroxy-3-thioacetic-1,4-naphthoquinone (JUGA) was synthesized in our laboratory, as described elsewhere. Acetaminophen, glycine and ascorbic acid were obtained from Sigma. All other reagents used were of analytical grade.

2.2. Methods

2.2.1. Electrode preparation

Glassy carbon (area 0.07 cm²) electrodes were polished prior to use on a polishing cloth (Struers, Denmark) with diamond pastes of decreasing size down to 1 μm. After electropolymerisation, the film coated-electrode was rinsed, then immersed for activation in a freshly prepared aqueous solution containing 0.03 M NHS and 0.015 M EDC during 2 h. After rinsing with distilled water, a 10 μL drop of freshly prepared enzyme solution of 5% w/w LOD in water was immediately delivered to the surface of the electrode. The enzyme was allowed to link overnight at 4 °C. The resulting electrode, called poly(JUG-co-JUGA)/LOD in the following, was then thoroughly washed with distilled water and stored at 4 °C before use.

2.2.2. Apparatus and procedure

A conventional 10 mL three-electrode cell was used, with a platinum auxiliary electrode and an Ag|AgCl wire reference electrode. A glassy carbon working electrode was used (*S*=0.07

cm²). The supporting electrolyte was 0.05 M phosphate buffer (pH 6) containing 0.05 M KCl. For amperometry tests, the thermostated cell (25 °C) was magnetically stirred 5s after each injection of lactate. Cell and lactate stock were bubbled with argon for at least 30 min and were blanketed with the inert gas for the duration of the experiment. When oxygen was used, the cell was kept under controlled oxygen partial pressure by controlling the ratio of argon and oxygen flows.

The spectrophotometric assay used to determine the enzymatic activity under the natural cosubstrate O₂ is based on the H₂O₂ production. This technique is routinely utilized since its first description [26].

2.3. Copolymer synthesis

The electrochemical synthesis of poly(JUG-co-JUGA) film was carried out by electrooxidation of a mixture of 5×10^{-2} M JUG + 5×10^{-3} M JUGA + 1×10^{-3} M 1-naphthol (as initiator of electropolymerisation) + 0.1 M LiClO₄ in acetonitrile, on GC electrodes, under dried argon atmosphere, by 25 potential scans at 50 mV s^{−1} between 0.4 and 1.05 V vs SCE, to obtain a 100 nm thick film (Fig. 1).

In the first stage, the current increases slowly with no significant modification of the overall signal characteristics. After this initial step (corresponding to 10–15 cycles), a noticeable variation of the voltammogram is observed with an anodic shift of the peak potential and an increase of the peak current.

The characterization of the polymer structure was based on data obtained previously in the study of the mechanism of 1-naphthol electropolymerization [27]. This has been thoroughly studied by the in situ Multiple Internal Reflection FTIR Spectroscopy (MIRFTIRS) technique [27]. Like many conjugated polymers, the chain growth occurs by successive steps including monomer oxidation to radical cations, dimer formation and chemical rearrangement. The dimerisation may be achieved by radical–radical or radical–substrate coupling. It was demonstrated [27] that the electropolymerisation of 1-naphthol occurs via successive radical–radical coupling and leads to an electro-

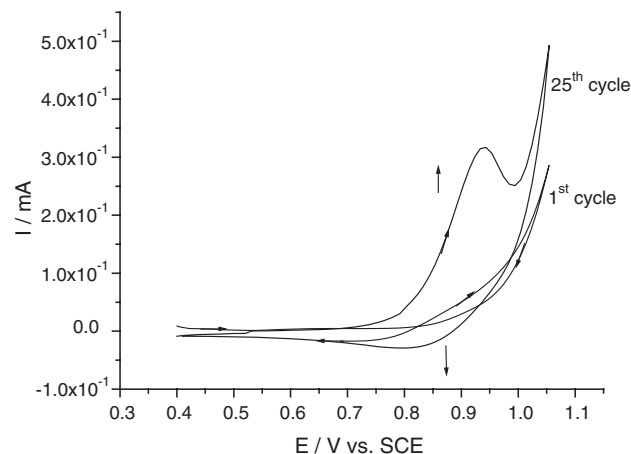


Fig. 1. First and last cyclic voltammograms corresponding to the electrooxidation of a mixture of 5×10^{-2} M JUG + 5×10^{-3} M JUGA + 1×10^{-3} M 1-naphthol + 0.1 M LiClO₄ in acetonitrile, on a GC electrode, under dried argon atmosphere. Scan rate: 50 mV s^{−1}.

Table 2
Main IR bands and their assignments for JUG, JUGA and poly(JUG-co-JUGA)

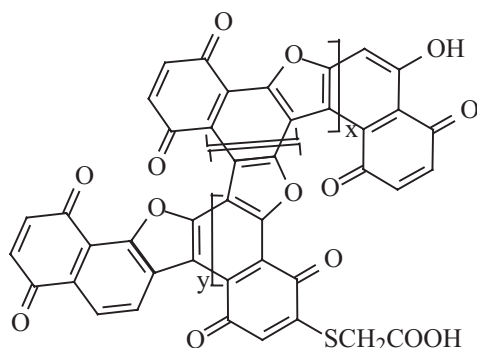
Band assignments	JUG/ cm ⁻¹	JUGA/ cm ⁻¹	Poly(JUG-co-JUGA)/ cm ⁻¹
ν O–H (as)	3431	3434	3521
ν O–H (s)	2924	–	–
ν C–H as (–S–CH ₂ –)	–	2975	3041
ν C–H s (–S–CH ₂ –)	–	2932	2935
ν C=O (COOH)	–	1716	1735
ν C=O (quinone)	1632	1641	1632
ν C=C (arom)	1665	1666	1668
(Naphthalene)	1591	1562	1597
ν C=C (arom) (furan)	–	–	1574
ν C–O–C (as) (furanne)	–	–	1290
ν C–O–C (s) (furanne)	–	–	1080
ν C–C (naphthalene)	1105	1105	1124
δ C–H out-of plane			
3H	752	759	–
2H	832	831	831
	856	856	864
1H	–	958	927
ClO ₄ ⁻	–	–	1081

active conducting polymer, poly(1-naphthol), constituted of alternated naphthalene and furan rings due to coupling occurring on the first nucleus following oxidation of the –OH group [27]. In that work (Ref. [27]), the concentration of the monomer used (1-naphthol) is 0.1 M and the potential applied is high.

In this work, 1-naphthol is added in low concentration (10^{-3} M) in order to initiate the polymerization. Indeed, we have checked this by performing the electrooxidation of 1-naphthol (10^{-3} M) alone in 0.1 M LiClO₄+acetonitrile. The resulting modified electrode presents no electrochemical activity in both acetonitrile and aqueous medium.

For the monomer used 5-hydroxy-1,4-naphthoquinone (JUG), we began by theoretical calculations based on frontier orbitals [28]. The data obtained showed that the radical–radical coupling proceeds similarly to the case of 1-naphthol., and does not affect the second nucleus bearing the quinone. The poly(JUG) structure was characterized by XPS and in situ FTIR spectroscopy.

After that, we extended the electrosynthesis to the case of the mixture juglone+JUGA (Fig. 1). Again, a thorough characterization of the copolymer structure was performed with in situ FTIR (during film growth) and ex situ FTIR after film formation. The main bands observed for the poly(JUG-co-JUGA) are summarized in Table 2 and the following structure is proposed for the copolymer.



Another evidence for this structure is afforded by the electroactivity of the quinone groups (Section 3.1).

The film shows a homogeneous and compact structure covered with scattered cauliflower features of regular size and distribution as usually observed for electrodeposited polymer [29]. An increase in the number of cycles results in a thicker film. We obtained a thickness of 100 nm after 25 cycles, and the following results will be related to this film thickness.

3. Results and discussion

Before investigations on the enzymatic activity of the bioelectrode, its fundamental electrochemical characteristics were studied. This would help to establish an overall kinetic mechanism.

3.1. Electroactivity

Quinone groups grafted on a polymer backbone, conductive or not, are known to have a poor electrochemical stability especially for the second redox couple involving the anion radical (QH^{•-}) and the dianion (Q²⁻). The electroactivity of the copolymer film poly(JUG-co-JUGA) was investigated in a 5×10^{-2} M phosphate buffer+ 10^{-2} M KCl (pH 6) (Fig. 2). The copolymer film shows a well-defined redox couple when cycled in the [–1 ; 0] V/SCE potential range. Both signals observed at –0.42 V/–0.55 V for the major redox couple, and that at –0.80/–0.87 V for shoulders are very stable upon cycling (several hundreds of cycles do not lead to any current decrease), which shows a remarkable electrochemical stability of the species involved in the charge transfer mechanism. This result could be explained by the original chemical structure of the polymer, especially for the quinone ring, which is fused with the polymer backbone and not only as pending group.

Under these conditions, voltammetry measurement at low scan rates allows to determine the total amount of electroactive quinones. Assuming that two electrons are exchanged per

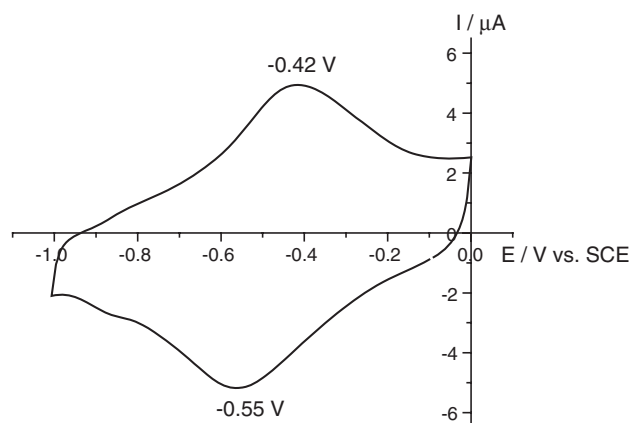


Fig. 2. Cyclic voltammogram of a poly(JUG-co-JUGA) film coated GC electrode, in the electroactivity domain of the quinone group. Scan rate 50 mV s^{-1} . Medium: 5×10^{-2} M K₂HPO₄/KH₂PO₄ buffer (pH 6)+ 10^{-2} M KCl (under argon atmosphere). Surface: 0.07 cm^2 . Film thickness: 100 nm. The electrode was previously equilibrated in the same medium by potential scanning between –1 and 0 V vs. SCE at 50 mV s^{-1} during 30 min.

quinone group, an apparent surface concentration of 8.10^{-10} mol cm $^{-2}$ was obtained.

3.2. Enzymatic activity of the electrode

The surface concentration of active enzyme immobilized onto the electrode surface has been determined by a spectrophotometric method described earlier [26]. Herein, this surface concentration is $\Gamma_E = 1.8 \times 10^{-12}$ mol cm $^{-2}$.

3.2.1. Amperometry

As evoked in the introduction section, LOD can be efficiently recycled by quinone (Table 1), at a lower working potential than for other common mediators. It is shown in the following that LOD can be recycled at a very low potential (-0.1 V vs. SCE), never reported in the literature. The enzymatic activity (and therefore the enzyme recycling) was evidenced by amperometric experiments upon lactate addition, on a poly(JUG-co-JUGA)/LOD electrode (see Experimental section).

Before each experiment, solutions (electrochemical cell and lactate stock) are deeply deaerated by argon bubbling. For the amperometric assay, the electrode is held at a constant working potential. After stabilization of the background current, successive aliquots of the stock lactate solution were injected and the solution magnetically stirred during ca. 5 s. The current increases immediately and reaches a plateau within ca. 100–200 s. On Fig. 3a is shown an example of amperometric test at -0.1 V vs. SCE., with enzyme (upper curve), and without enzyme (blank, lower case). A blank experiment was also made with injection of hydrogen peroxide. No current was detected.

The calibration plot (Fig. 3b) shows a Michaelis-shaped curve, with two well-defined regimes: the linear part defined by an initial rate of ca. $70 \mu\text{A M}^{-1} \text{cm}^{-2}$, an apparent K_m^{app} of ca. 1.5 mM, and the saturation part with a maximum rate of ca. $0.17 \mu\text{A cm}^{-2}$. The linear range starts at about $50 \mu\text{M}$ (which is the detection limit) and ends at $1500 \mu\text{M}$. In the literature, sensitivities are sometimes higher, but acquired at the price of higher potentials.

Stirring has no influence on the current, in this concentration range (0–20 mM). Experiments were performed on a rotating disk electrode, at various rotation speeds between 100–3600 Hz. No measurable increase or decrease of the current was observed. This means that the overall process is not limited by diffusion of reactants towards the electrode.

3.2.2. Working potential

For a constant lactate concentration of 20 mM (i.e., under the saturation regime), the working potential was varied between -0.1 V and $+0.3$ V vs. SCE. The experiments were performed on the same electrode to avoid deviation from one electrode to another. For each point, the background current was subtracted (Fig. 4). It is clear that the current increases sharply around -0.1 V, to stabilize after $+0.2$ V. Considering this curve, it could be surprising, in a first approach, to choose -0.1 V as the best working potential for the system. However,

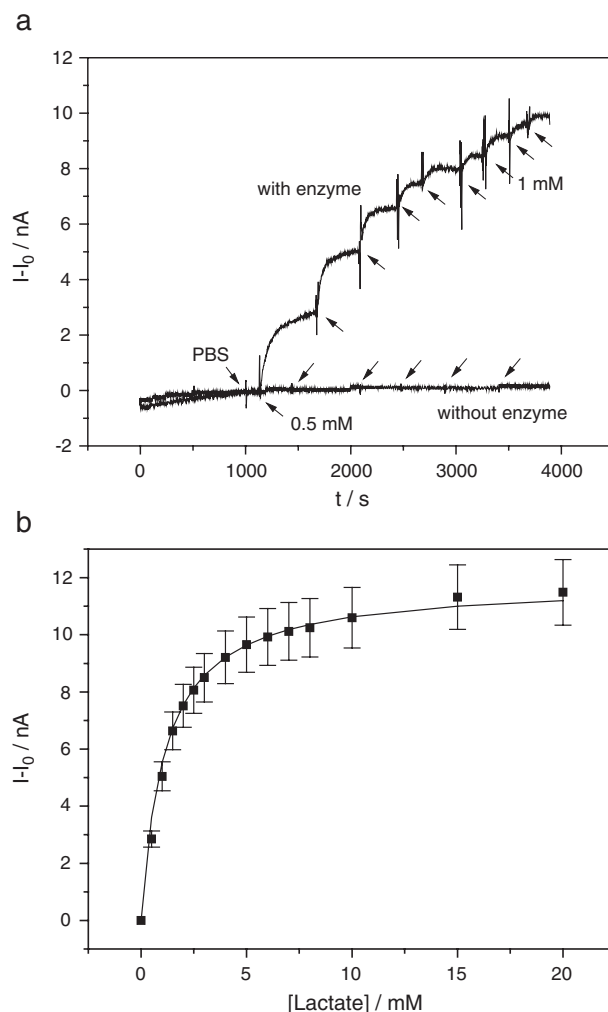


Fig. 3. a: Upper curve : amperometric response for a GC/poly(JUG-co-JUGA)/LOD electrode versus time. $E = -0.1$ V vs. SCE. Medium: 5×10^{-2} M $\text{K}_2\text{HPO}_4/\text{KH}_2\text{PO}_4$ buffer (pH 6) + 10^{-2} M KCl (under argon atmosphere). Surface: 0.07 cm^2 . Film thickness: 100 nm. Temperature: 25°C . Lactate is added to raise the concentration by steps of 0.5 mM (6 first injections), then 1 mM. I_0 is the background current before the first injection. Lower curve : amperometric response for a GC/poly(JUG-co-JUGA) electrode (without enzyme), in the same conditions as above. b: Calibration plots for the GC/poly(JUG-co-JUGA)/LOD electrode versus lactate concentration. Same conditions as Fig. 3a. Lactate is added to raise the concentration by steps of 0.5 mM (6 first injections), then 1 mM (5 following injections), 2 mM and 5 mM. The solid line corresponds to a numerical fit from expression XII.

as will be discussed in Section 3.4., this value is the best compromise, sufficiently low to avoid side reactions with interferents.

3.2.3. pH

The pH effect is, in this system, very interesting and unusual. Indeed, LOD is known to present in homogeneous conditions a maximum of activity around pH 6. The interesting point is that the apparent enzyme activity measured by the current flow through the electrode here varies differently. Indeed, the current increases continuously with pH, from pH 5 to pH 10 (Fig. 5).

After immobilization on a substrate, the enzymatic activity is likely to vary significantly for two main reasons: deactiva-

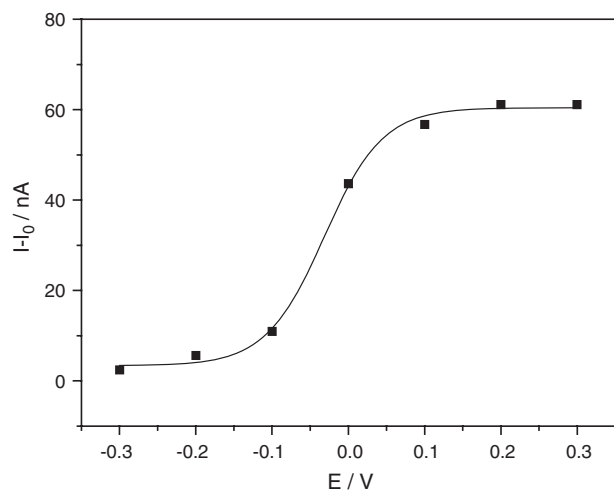


Fig. 4. Current intensities for a GC/poly(JUG-co-JUGA)/LOD electrode under the same conditions as in Fig. 3, at saturation of substrate (20 mM lactate), as a function of the working potential. The background current I_0 was measured for each potential, before addition of lactate. The plain line is only a visual guide.

tion coming from denaturation, or due to local pH effect. This latter point was investigated by a spectrophotometric method (see Experimental section). pH was varied between 5 and 8. The apparent activity (measured by the H_2O_2 producing rate) was reported vs. pH (not shown). As expected, a bell-shaped curve was obtained, with a maximum at pH 7, i.e., slightly shifted in comparison to homogeneous conditions. This could be explained as follows: under aerobic conditions, protons coming from the substrate are accepted by O_2 (to form H_2O_2), so the pH does not vary.

On the contrary, when quinones (Q) are used, protons intervene in the redox process so that the local pH can be varied.

3.2.4. Temperature effect

The effect of temperature changes was also monitored. As for pH, temperature effects can be decomposed into two

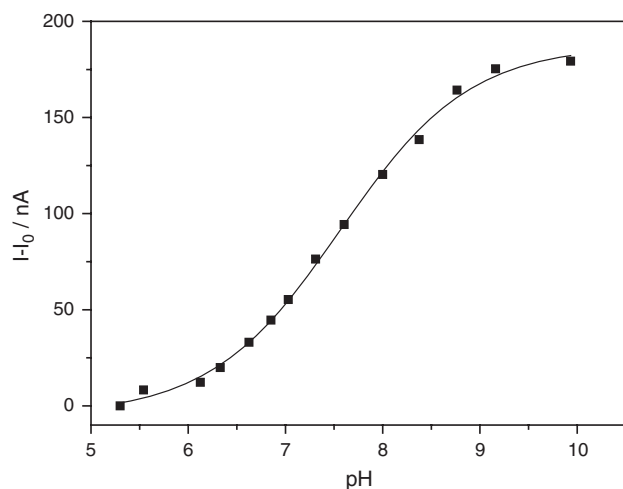


Fig. 5. Current intensities for a GC/poly(JUG-co-JUGA)/LOD electrode under the same conditions as in Fig. 3, at saturation of substrate (20 mM lactate), as a function of the pH (measured in the bulk). The background current I_0 was measured for each potential, before addition of lactate. The plain line is only a visual guide.

processes. On one hand, a temperature increase leads to an increase of the reaction rate following the Arrhenius law. On the other hand, enzyme denaturation occurs, for temperatures above ca. 40 °C. This is well illustrated by the results reported in Fig. 6. At saturation of substrate (20 mM), applying the Arrhenius law between 20 and 40 °C gives an activation energy of $E_a = 68.3 \text{ kJ mol}^{-1}$. This value corresponds to data in the literature [30] for this enzyme. To avoid any risk of denaturation, most of the experiments reported in this paper were performed at 25 °C.

3.2.5. Stability of the amperometric response

Amperometric measurements were performed on the same electrode for several experiments during 9 weeks. Between the assays the bioelectrode was kept in PBS solution at 4 °C. After a burst during the 3 first uses of the electrode (where some enzymes are probably lost in solution) corresponding to a signal decrease of ca. 50%, the sensitivity stabilizes around $70 \mu\text{A M}^{-1} \text{ cm}^{-2}$, with a mean deviation of $\pm 10 \mu\text{A M}^{-1} \text{ cm}^{-2}$. No sign of deactivation appears within 9 weeks.

3.3. Elements of kinetic

The kinetic pathway for this bioelectrode is complex. Indeed, two main steps are involved: the enzyme kinetic, and the polymer kinetic. It could be quite difficult to separate and identify each step. The point that is particularly interesting here is the enzyme/quinone recycling kinetic. To investigate this step, the idea herein is to study the interference between reoxidation by quinone and by molecular oxygen.

Dioxygen is the natural cosubstrate of LOD and can interfere with the quinone-mediated reaction pathway (Scheme 1). Actually, this interference is due to a competition between the artificial mediator (quinone) and the natural cosubstrate

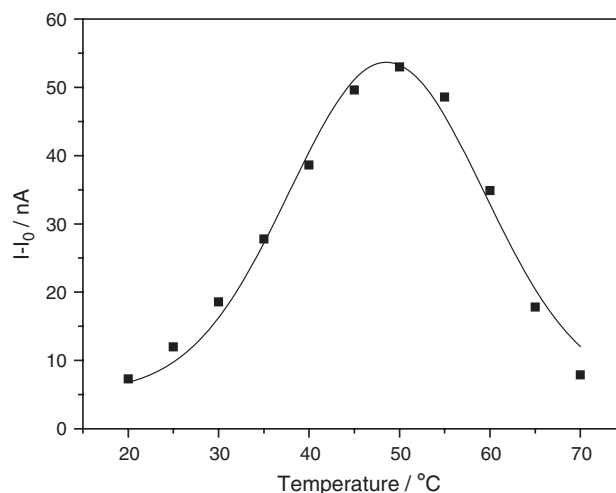
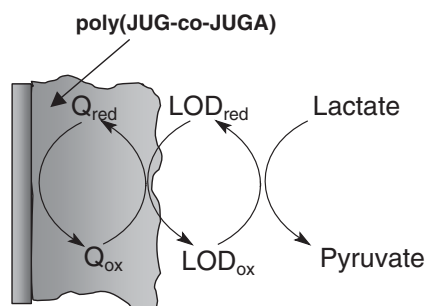


Fig. 6. Current intensities for a GC/poly(JUG-co-JUGA)/LOD electrode under the same conditions as in Fig. 3, at saturation of substrate (20 mM lactate), as a function of temperature. A preliminary experiment has shown that the background current I_0 (current without lactate) does not vary with temperature. The plain line is only a visual guide.



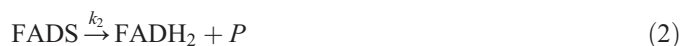
Scheme 1. Schematic representation of the reaction pathway, when quinone (Q) immobilized in poly(JUG-co-JUGA) film is used as an artificial mediator.

(dioxygen) to regenerate the oxidized form of the active center FAD, as illustrated on Scheme 2.

Kowning the recycling kinetic with oxygen, it is thus possible to estimate the recycling kinetic with quinone. To simplify the model, polarisation effects through the film is not considered. In addition, the active fraction of the mediator through the film is not homogeneous either. But this method should allow to obtain averaged values that are significant.

3.3.1. Without oxygen

With the artificial mediator quoted M_{ox} (oxidized state) or M_{red} (reduced state), the kinetic pathway is described as follows:



The global reaction rate is calculated considering the quasi-stationary hypothesis, for the intermediate products. Details are skipped, to give directly the expression of the current collected to the electrode. With the quinone group as the mediator, Γ_Q

the quinone surface concentration and A the electrode surface, we obtain:

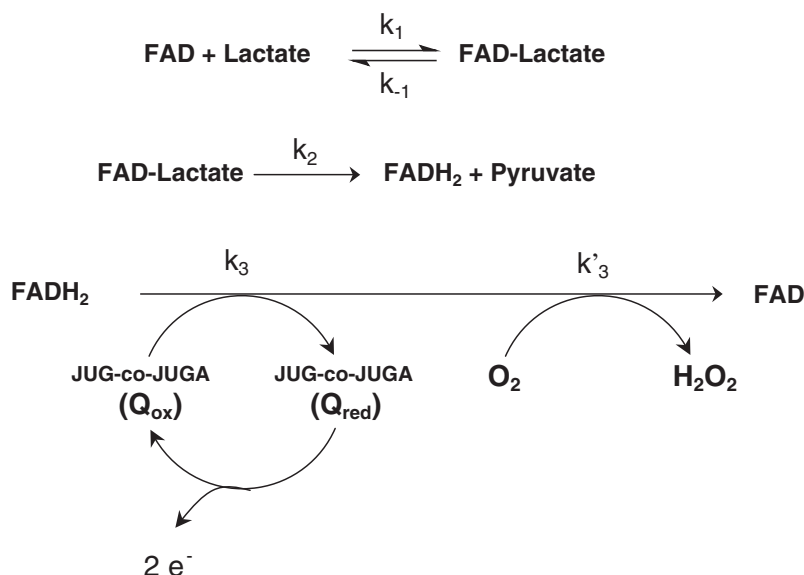
$$\frac{1}{i} = \frac{1}{2FA\Gamma_E} \left[\frac{1}{k_2} + \frac{1}{k_3\Gamma_Q} + \frac{1}{k_1[S]} + \frac{k_{-1}}{k_1k_2[S]} \right] \quad (I)$$

3.3.2. With oxygen

In an aerated medium, the enzyme recycling by quinone competes with the oxygen pathway. It should be mentioned that quinone is known to catalyze the $2e^- O_2$ reduction. This reaction was envisaged, but is discarded herein. Indeed, cyclic voltammetry was performed on the modified electrode in aerobic conditions, and it appears that the catalytic reduction current is negligible. The new pathway with oxygen is shown below:



Experimentally, to estimate the effect of dissolved oxygen, amperometric experiments were performed under the same conditions as in Section 3.2.1. (GC electrode, working potential of -0.1 V vs. Ag|AgCl), but in a medium for which partial O_2 pressure was varied from 0 up to 100%, at saturation of substrate (20 mM). Oxygen concentration in water follows Henry's law. At $25^\circ C$, $K_{O_2} = 3.30 \times 10^7 \text{ torr}^{-1}$. Therefore, P_{O_2} corresponds to a concentration range of 0 to $1.28 \times 10^{-3} \text{ mol L}^{-1}$ ($2.6 \times 10^{-4} \text{ mol L}^{-1}$ at 20% O_2), that is reported on Fig. 7. O_2 has, in a first approach, a negligible effect for partial pressures lower than 20% (less than 5% decrease), and half of the initial current is still observed under 60% O_2 .



Scheme 2. Enzymatic reaction pathway illustrating the competitive recycling of FAD group by quinone on one hand and dioxygen on the other hand.

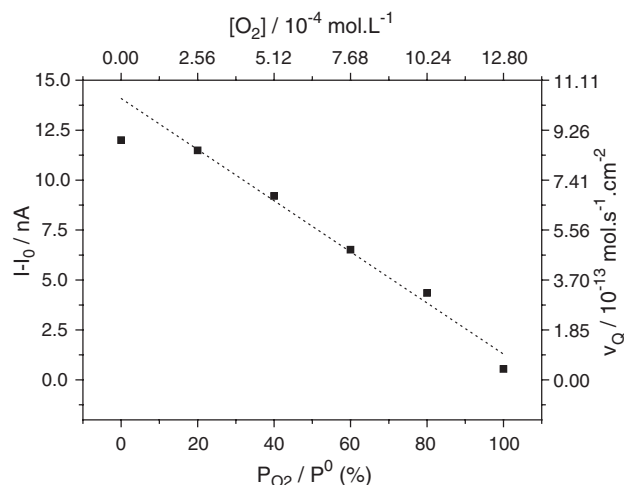


Fig. 7. Current intensities for a GC/poly(JUG-co-JUGA)/LOD electrode under the same conditions as in Fig. 3, at saturation of substrate (20 mM lactate), as a function of the relative O_2 partial pressure in the electrochemical cell (after a 30 min equilibration). 0% corresponds to pure argon. I_0 does not vary with P_{O_2} .

For a better understanding of the process, two experiments were performed on a same electrode. First, via the spectrophotometric method described earlier, the enzymatic activity of the electrode was measured when the natural cosubstrate O_2 is used. In this case, quinones do not participate to the recycling of lactate oxidase. Fig. 8 reports the quantity of H_2O_2 produced versus time, at saturation of substrate (20 mM). The reaction rate, calculated from the slope of the interpolated line, gives:

$$v_{O_2} = \frac{dn_{H_2O_2}}{dt} = \frac{dn_{FADH_2}}{dt} = 4.29 \times 10^{-12} \text{ mol s}^{-1} \text{ cm}^{-2},$$

for an O_2 partial pressure of 20%.

In a second experiment, the bioelectrode was polarized at -0.1 V in deaerated medium to measure the activity was measured of quinone as mediator. For the same lactate concentration as above (20 mM), the measured current is $I_Q = 12$ nA. Therefore, the reaction rate is:

$$v_Q = \frac{1}{nFA} i_Q = \frac{dn_{FADH_2}}{dt} = 8.89 \times 10^{-13} \text{ mol s}^{-1} \text{ cm}^{-2},$$

with $n = 2$.

These results are interesting to compare. Indeed, it is shown on one hand that O_2 does not compete much with Q (Fig. 7), and on the other hand, that $v_{O_2} > v_Q$ (for the same O_2 partial pressure in both cases). It seems to be a contradiction. This can be explained considering that the electrical “wiring” of LOD is not homogeneous in the whole film. A fraction of LOD is probably more efficiently recycled by quinone than by O_2 (i.e., insensitive to O_2) while the other fraction is regenerated more easily with O_2 . This behavior, depending for example on the enzyme orientation onto the electrode surface, is described in the literature [16].

In the case where the substrate S is added in large excess ($[S] \rightarrow \infty, \gg K_m$), and with the hypothesis that the enzyme recycling is the limiting step, i.e., $k_2 \gg k_3 \Gamma_Q$ and $k_2 \gg k'_3 [O_2]^*$ (* for $[O_2]$ at the surface of the electrode), we can write from

(XI) the regeneration rates of the enzyme by quinone (v_Q) or oxygen (v_{O_2}):

$$v_Q = k_3 \Gamma_Q \Gamma'_E \text{ and } v_{O_2} = k'_3 [O_2]^* \Gamma'_E$$

with Γ'_E the surface concentration of LOD that is electrically connected with quinone. If x is the fraction of enzymes that is connected, $\Gamma'_E = x \Gamma_E$.

If there is competition between Q and O_2 for enzyme reoxidation, the new regeneration rate v'_Q of the enzyme by quinone is approximately:

$$v'_Q = k_3 \Gamma_Q \Gamma'_E - k'_3 [O_2]^* \Gamma'_E$$

Thus, $v'_Q = v_Q - x k'_3 \Gamma_E [O_2]^*$ (II)

(II) is the equation of a straight line, with v_Q as the origin for 0% O_2 , and $-x k'_3 \Gamma_E$ as the negative slope. This fits very correctly the results of Fig. 7, except for low O_2 pressure. This deviation could be due to residual O_2 , i.e., 0% does not correspond to a thoroughly deaerated medium. Extrapolation of the straight line to 0% O_2 gives the “true” v_Q . We found (see Fig. 7) 115% at 0% O_2 . We know also absolute values for v_Q and v_{O_2} , measured above for 20% O_2 , $8.89 \times 10^{-13} \text{ mol s}^{-1} \text{ cm}^{-2}$ and $4.29 \times 10^{-12} \text{ mol s}^{-1} \text{ cm}^{-2}$, respectively. Therefore, with (II):

$$v'_Q = 1.15 \times 8.89 \times 10^{-13} - x \times 4.29 \times 10^{-12} \text{ and} \\ v'_Q = 0.95 v_Q \text{ for } 20\% O_2$$

$$\text{Thus, } v'_Q = 1.02 \times 10^{-12} - x \times 4.29 \times 10^{-12} \\ = 0.95 \times 8.89 \times 10^{-13}$$

We deduce that $x = 0.04$. This means that $\Gamma'_E = 0.04 \Gamma_E$, i.e., that 4% of the immobilized active enzymes are electrically connected to quinone groups.

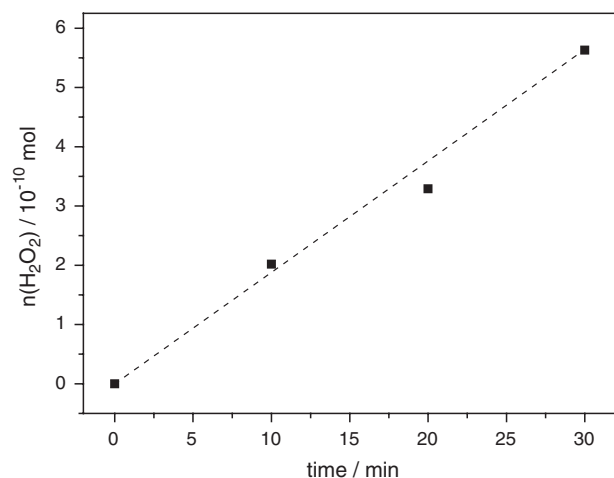


Fig. 8. Quantity of H_2O_2 produced versus time, at saturation of substrate (20 mM lactate), for a GC/poly(JUG-co-JUGA)/LOD electrode. Medium: 5×10^{-2} M K_2HPO_4/KH_2PO_4 buffer (pH 6) + 10^{-2} M KCl (under argon atmosphere). Surface: 0.07 cm^2 . Film thickness: 100 nm. Temperature: 25°C . The dashed line is a visual guide.

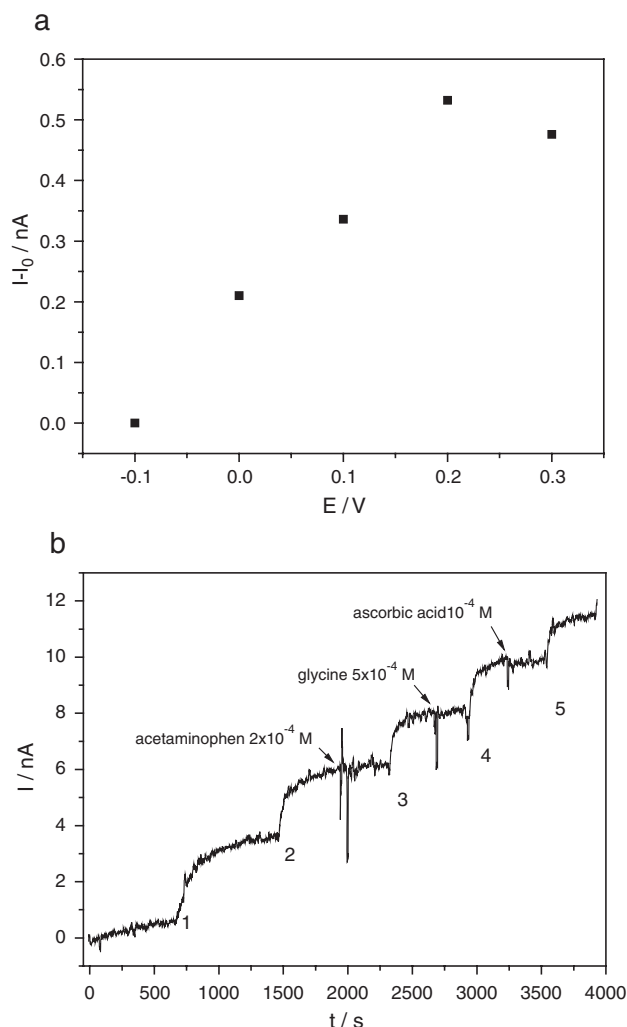


Fig. 9. (a) Ascorbic acid ($2 \cdot 10^{-4}$ M) oxidation current as a function of potential, on a GC/poly(JUG-co-JUGA) electrode. Medium: 5×10^{-2} M $\text{K}_2\text{HPO}_4/\text{KH}_2\text{PO}_4$ buffer (pH 6) + 10^{-2} M KCl (under argon atmosphere). Surface: 0.07 cm^2 . Film thickness: 100 nm. Temperature: 25°C . (b) Amperometric response of the same electrode at -0.1 V/SCE , for successive injections of $5 \cdot 10^{-4} \text{ M}$ lactate (inject. 1 to 5), combined with addition of interferents (inject. 2 to 4, acetaminophen, glycine and ascorbic acid, respectively). Same conditions as (a).

The slope of the straight line of Fig. 7 ($7.97 \times 10^{-10} \text{ L s}^{-1} \text{ cm}^{-2}$) can also give the kinetic constant k'_3 . Indeed, this slope equals to $-x k'_3 \Gamma_E$, with x and Γ_E which are known.

$$x k'_3 \Gamma_E = 7.97 \times 10^{-10} \text{ L s}^{-1} \text{ cm}^{-2} \Rightarrow k'_3 = 9.96 \times 10^3 \text{ L mol}^{-1} \cdot \text{s}^{-1}$$

We can also characterize the recycling kinetic via the quinone group, with $k_3 \Gamma_Q$.

$$\begin{aligned} v_Q &= 1.15 \times 8.89 \times 10^{-13} \text{ and} \\ v_Q &= k_3 \Gamma_Q \Gamma'_E \Rightarrow k_3 \Gamma_Q = 1.02 \times 10^{-12} / x \Gamma'_E \Rightarrow k_3 \Gamma_Q \\ &= 1.02 \times 10^{-12} / (4 \cdot 10^{-2} \times 2 \cdot 10^{-12}) = 12.75 \text{ s}^{-1} \end{aligned}$$

It appears that this value, when replaced in expression (I), allows to fit nicely the experimental points (Fig. 3b, plain line),

with these parameters: $\Gamma_E = 1.8 \times 10^{-12} \text{ mol cm}^{-2}$ (as found by the spectrophotometric method); $A = 0.07 \text{ cm}^2$; $F = 96490 \text{ C mol}^{-1}$; $k_2 = 266 \text{ s}^{-1}$ [31]; $k_1 = 5.09 \times 10^{-4} \text{ L mol}^{-1} \text{ s}^{-1}$ [31]; $k_{-1} = 10^3 \text{ s}^{-1}$ [31]; $k_3 \Gamma_Q = 12.75 \text{ s}^{-1}$ (as found above).

3.4. Complex samples

It was shown in Section 3.2.2 that the working potential of the poly(JUG-co-JUGA)/LOD system can be very low. Therefore, most of the well-known side-oxidations can be avoided, as demonstrated below.

First, we have performed oxidation of ascorbic acid (one of the most common interferences) on the modified electrode at various potentials. Ascorbic acid begins to be oxidized at 0 V vs. SCE and obviously at higher potentials (Fig. 9a). This justifies our choice of -0.1 V vs. SCE as the working potential. The other interferences are oxidized at higher potentials.

On Fig. 9b is presented an amperometric curve obtained at -0.1 V for successive additions of lactate combined with addition of some interferences as acetaminophen, glycine and ascorbic acid. As it is shown, none of these chemicals interfere noticeably with the current due to enzyme recycling.

As an illustration of the reliability of this electrode, an amperometric test was performed on a commercial sample: yogurt. Yogurts contain lactic acid, coming from the fermentation process, and its concentration is carefully monitored for commercialization. The experiment was conducted as follows (Fig. 10): two plots (a, b) were first obtained by successive additions of lactate (0.2 mM each). Then 50 mg of yogurt were added, without any pretreatment, directly in the electrochemical cell, and the solution stirred vigorously. The current increased up to 4.9 nA. After stabilization, plot d (6.6 nA) was obtained by addition of lactate (0.2 mM). The 3 points (a, b, d) make a straight line. The lactate concentration can then be

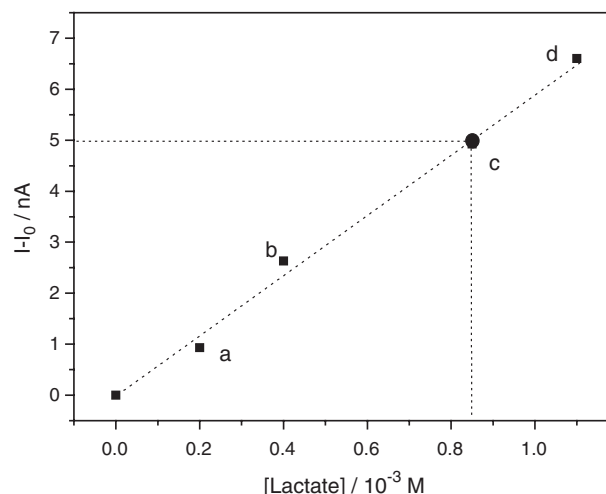


Fig. 10. Data from amperometric test for a GC/poly(JUG-co-JUGA)/LOD electrode with a commercial food-industry sample. The plain squares correspond to addition of $2 \times 10^{-4} \text{ M}$ lactate, under the same conditions as in Fig. 3. The third point (open circle) corresponds to addition of 50 mg of yogurt in the electrochemical cell. The yogurt sample was directly added in the cell without any filtration.

deduced : a current of 4.9 nA gives 0.85 mM (point C). This shows that the commercial sample presents a lactate concentration of $0.85 - 0.4 = 0.45$ mM in the 10-mL cell, i.e., around 0.1 mmol per g. of yogurt, which is the value claimed by the manufacturer. Therefore, this result illustrates that the poly(-JUG-co-JUGA)/LOD electrode seems to be reliable for this kind of test with a complex sample containing other constituents than lactate. Obviously, this result deserves to be extended to other complex samples, but this is not the objective of this work.

4. Conclusion

In this paper, we present the development of a reagentless amperometric lactate biosensor based on a novel functionalized conducting polymer. The electroactivity of the quinone embedded in the polymer structure is remarkably stable in neutral aqueous medium. The enzyme kinetic, and more precisely the recycling step, was investigated, showing that quinone group can act as a very efficient electron acceptor for lactate oxidase (LOD) recycling at very low working potential. This interesting performance allows to avoid interfering currents. This biosensor can be used in very practical conditions, e.g., on a commercial sample. Work is in progress to exploit our system with other oxidase enzymes.

References

- [1] W. Matuszewski, M. Trojanowicz, Graphite paste-based enzymatic glucose electrode for flow injection analysis, *The Analyst* 113 (1988) 735.
- [2] S.J. Updike, G.P. Hicks, Enzyme electrode, *Nature* 214 (1967) 986–988.
- [3] E. Csöregi, C.P. Quinn, D.W. Schmidtke, S.E. Lindquist, M.V. Pishko, L. Ye, I. Katakis, J.A. Hubbell, A. Heller, Design, characterization, and one-point in vivo calibration of a subcutaneously implanted glucose electrode, *Anal. Chem.* 66 (1994) 3131–3138.
- [4] G.J. Leggett, C.J. Roberts, P.M. Williams, M.C. Davies, D.E. Jackson, S.J.B. Tendler, Approaches to the immobilization of proteins at surfaces for analysis by scanning tunneling microscopy, *Langmuir* 9 (1993) 2356–2362.
- [5] Y. Miao, J. Chen, X. Wu, Using electropolymerized non-conducting polymers to develop enzyme amperometric biosensors, *Trends Biotech.* 22 (2004) 227–231.
- [6] J.C. Vidal, E. Garcia, J.R. Castillo, In situ preparation of overoxidized PPy/oPPD bilayer biosensors for the determination of glucose and cholesterol in serum, *Sens. Actuators, B, Chem.* 57 (1999) 219–226.
- [7] M. Situmorang, J.J. Gooding, D.B. Hibbert, D. Barnett, Electrodeposited polytyramine as an immobilisation matrix for enzyme biosensors, *Biosens. Bioelectron.* 13 (1998) 953–962.
- [8] W. Schuhmann, Conducting polymer based amperometric enzyme electrodes, *Mikrochim. Acta* 121 (1995) 1–29.
- [9] M. Umana, J. Waller, Protein-modified electrodes. The glucose oxidase/polypyrrole system, *Anal. Chem.* 58 (1986) 2979–2983.
- [10] N.C. Foulds, C.R. Lowe, Enzyme entrapment in electrically conducting polymers. Immobilization of glucose oxidase in polypyrrole and its application in amperometric glucose sensors, *J. Chem. Soc., Faraday Trans.* 82 (1986) 1259–1264.
- [11] P.N. Bartlett, R.G. Whitaker, Electrochemical immobilization of enzymes. Part II: Glucose oxidase immobilized in poly-*n*-methylpyrrole, *J. Electroanal. Chem.* 224 (1987) 37–48.
- [12] S. Cosnier, Biomolecule immobilization on electrode surfaces by entrapment or attachment to electrochemically polymerized films. A review, *Biosens. Bioelectron.* 14 (1999) 443–456.
- [13] C. Godet, M. Boujtita, N. El Murr, Direct electron transfer involving a large protein: glucose oxidase, *New J. Chem.* 23 (1999) 795–797.
- [14] L. Gorton, E. Dominguez, Electrocatalytic oxidation of NAD(P) H at mediator-modified electrodes, *Rev. Mol. Biotechnol.* 82 (2002) 371–392.
- [15] P. De Taxis du Poet, S. Miyamoto, T. Murakami, J. Kimura, I. Karube, Direct electron transfer with glucose oxidase immobilized in an electro-polymerized poly(*N*-methylpyrrole) film on a gold microelectrode, *Anal. Chim. Acta* 235 (1990) 255–263.
- [16] W. Schuhmann, Amperometric enzyme biosensors based on optimized electron-transfer pathways and non-manual immobilization procedures, *Rev. Mol. Biotechnol.* 82 (2002) 425–441.
- [17] K. Habermüller, M. Mosbach, W. Schuhmann, Electron-transfer mechanisms in amperometric biosensors, *Fresenius' J. Anal. Chem.* 366 (2000) 560–568.
- [18] J.J. Kulys, N.K. Cenas, Oxidation of glucose oxidase from *Penicillium vitale* by one- and two-electron acceptors, *Biochem. Biophys. Acta* 744 (1983) 57–63.
- [19] T.J. Ohara, R. Rajagopalan, A. Heller, Wired enzyme electrodes for amperometric determination of glucose or lactate in the presence of interfering substances, *Anal. Chem.* 66 (1994) 2451–2457.
- [20] G. Kenausis, C. Taylor, R. Rajagopalan, A. Heller, Wiring of lactate oxidase within a low-redox potential electron-conducting hydrogel, *J. Mol. Recognit.* 9 (1998) 626–630.
- [21] E. Corton, F. Battaglini, Effect of milk proteins on the behavior of a biosensor based on poly(allylamine) containing an osmium complex wired to redox enzymes Part 1. Monoenzymatic configuration, *J. Electroanal. Chem.* 511 (2001) 1–7.
- [22] A. Chaubey, B.D. Malhotra, Mediated biosensors, *Biosens. Bioelectron.* 17 (2002) 441–456.
- [23] G. Arai, M. Masuda, I.Y. Yasumori, Glucose sensor of poly(mercapto-*p*-benzoquinone) films containing immobilized glucose oxidase, *Chem. Lett.* (1992) 1791–1794.
- [24] G. Arai, T. Noma, M. Hayashi, I. Yasumori, Electrochemical characteristics of D-amino acid oxidase immobilized in a conductive redox polymer, *J. Electroanal. Chem.* 452 (1998) 43–48.
- [25] J. Haccoun, B. Piro, L.D. Tran, L.A. Dang, M.C. Pham, Reagentless amperometric detection of L-lactate on an enzyme-modified conducting copolymer poly(5-hydroxy-1,4-naphthoquinone-co-5-hydroxy-3-thioacetic acid-1,4-naphthoquinone), *Biosens. Bioelectron.* 19 (2004) 1325–1329.
- [26] R.E. Childs, W.G. Bardsley, The steady-state kinetics of peroxidase with 2,2'-azino-di-(3-ethyl-benzthiazoline-6-sulphonic acid) as chromogen, *Biochem. J.* 145 (1975) 93–103.
- [27] M.C. Pham, J. Moslih, P.C. Lacaze, Synthesis and characterization of a new conducting electropolymerized film from 1-naphthol, *J. Electrochem. Soc.* 138 (1991) 449–454.
- [28] B. Piro, J. Haccoun, M.C. Pham, L.D. Tran, A. Rubin, H. Perrot, C. Gabrielli, Study of the DNA hybridization transduction behavior of a quinone-containing electroactive polymer by cyclic voltammetry and electrochemical impedance spectroscopy, *J. Electroanal. Chem.* 577 (2005) 155–165.
- [29] T.A. Skotheim, R.L. Elsenbaumer, J.R. Reynolds (Eds.), *Handbook of Conducting Polymers*, 2nd ed., 1997, p. 484.
- [30] S. Ghisla, V. Massey, Studies on the mechanism of action of the flavoenzyme lactate oxidase. Proton uptake and release during the binding of transition state analogs, *J. Biol. Chem.* 252 (1977) 6729–6735.
- [31] K. Maeda-Yorita, K. Aki, H. Sagai, H. Misaki, V. Massey, L-lactate oxidase and L-lactate monooxygenase: mechanistic variations on a common structural theme, *Biochimie* 77 (1995) 631–642.